Supplementary Information (SI) for Soft Matter.

SUPPORTING INFORMATION

Ion effects on minimally hydrated polymers: hydrogen bond populations and dynamics

Eman Alasadi[1] and Carlos R. Baiz[1,*]

Department of Chemistry, University of Texas at Austin, 105 E 24th St. A5300, Austin, TX 78712, USA
corresponding author: cbaiz@cm.utexas.edu

SI.1 Hydrogen Bond Populations

FTIR spectra were measured at 1 cm^{-1} resolution using a Bruker Vertex 70 FTIR spectrometer. Each spectrum is an average of 32 scans from 400 to 4000 cm^{-1} measured at room temperature. Spectra were background-subtracted with a D_2O solvent spectrum measured under the same conditions. To analyze the measured FTIR data, the ester C=O stretching spectra are fit to a sum of two Gaussians (**Eq. 1**):

$$A(\omega) = \sum_{n=1}^{2} a_n e^{\frac{-(\omega - b_n)^2}{2c_n}} \quad (1)$$

In this equation, A(ω) represents the absorbance at a given frequency ω, while a, b, and c correspond to the amplitude, center frequency, and width of each Gaussian peak, respectively. The peak areas, which are indicative of the hydrogen bond populations, are calculated based on these parameters.

The distinct shapes and positions of the peaks in the FTIR spectra reflect the distribution of hydrogen bonding populations within the polymer matrix. These variations indicate different environments of the carbonyl groups, either free or hydrogen-bonded. The fitting process deconvolutes these overlapping spectral features, attributing each Gaussian component to a specific hydrogen bonding state, and the relative intensities and positions of the fitted peaks provide insight into the hydrogen bond populations present in each system. As a note, previous work[1] has quantified the changes in the ester carbonyl transition dipole moment with respect to the hydrogen bond population. The changes are approximately 13% higher for the 1 hydrogen bond compared to the 0 hydrogen bond.

Further, peak area correlates to the population of the individual hydrogen-bond (H-bond) species. Peak 1 (highest frequency) is the 0 H-bond population and peak 2 (~15 cm^{-1} red-shifted) is the 1 H-bond population. To obtain peak area, fitting was performed using a nonlinear least squares method with bisquare robust weighting to minimize the influence of outliers. During this fitting process, the parameters a, b, and c are optimized to best match the experimental data. The uncertainties in these parameters, which are reflected in the error bars, are derived from the covariance matrix produced during the fitting process. The diagonal elements of this matrix provide the variances of the fitted parameters, and the square roots of these variances give the standard deviations, which are used as the error bars.

To ensure the quality and accuracy of the fit, the second derivative of the absorbance with respect to frequency was also plotted, helping to verify the correctness of the fitted peak positions. These error bars thus represent the confidence intervals around the hydrogen bond populations and provide a quantitative measure of the uncertainty in the fitting process.

All FTIR data analysis was performed using the MATLAB R2021b package of programs. To verify the quality of our results, we plot the total fit, the original spectrum, and their second derivative of absorbance with respect to frequency. These are provided in Figures S1-S6.

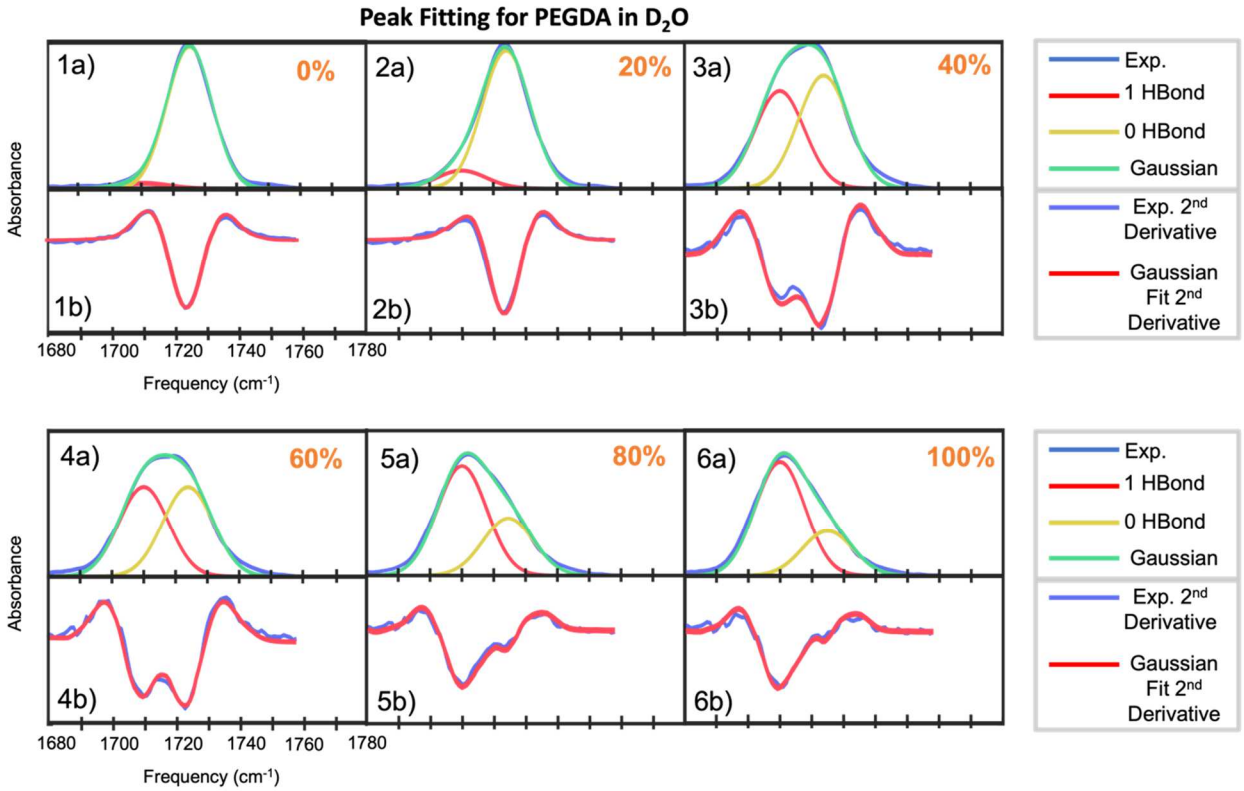

Figure 1. Sample fit (a) and the corresponding second derivative (b) for polymer PEGDA in D_2O for varying weight %. Here, panel 1 is for 0%, panel 2 is for 20%, panel 3 is for 40%, panel 4 is for 60%, panel 5 is 80%, and panel 6 is 100%. In the top section of each panel, the original FTIR spectrum is shown in blue, the sum of the two-Gaussian fit is shown in green, and the 0 and 1 H-bond populations are shown in yellow and red respectively. The bottom panel displays the original FTIR spectrum second derivative in blue and the fitted spectrum is represented in red.

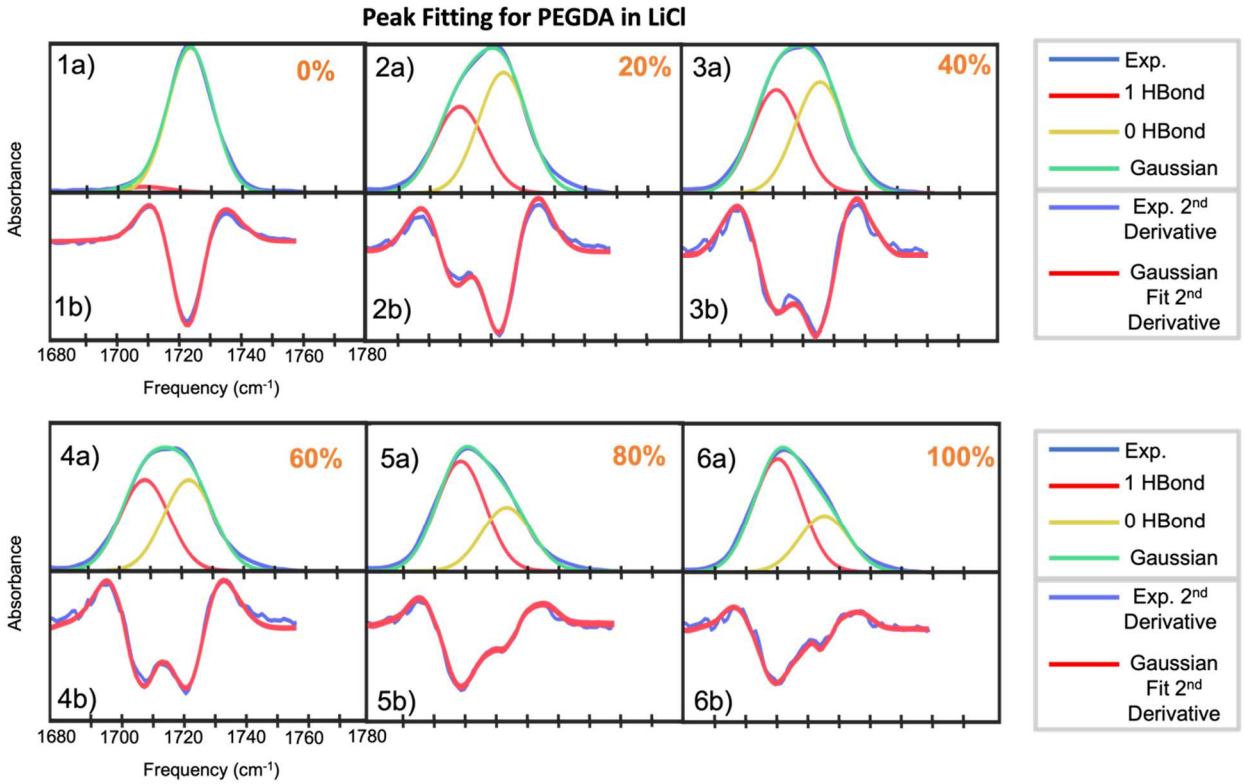

Figure 2. Sample fit (a) and the corresponding second derivative (b) for polymer PEGDA in D_2O with LiCl for varying weight %. Here, panel 1 is for 0%, panel 2 is for 20%, panel 3 is for 40%, panel 4 is for 60%, panel 5 is for 80%, and panel 6 is for 100%. In the top section of each panel the original FTIR spectrum is shown in blue, the sum of the two-Gaussian fit is shown in green, the 0 and 1 H-bond populations are shown in yellow and red respectively. The bottom panel displays the original FTIR spectrum second derivative in blue and the fitted spectrum is represented in red.

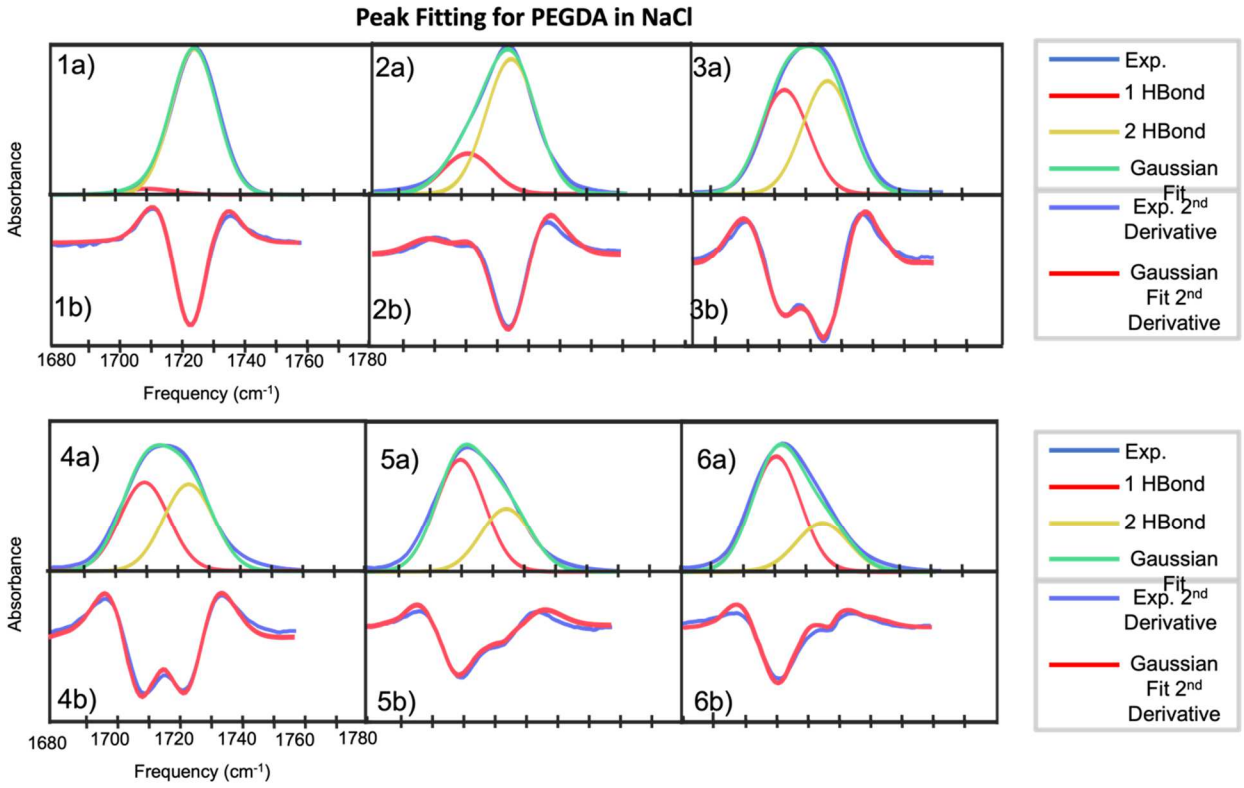

Figure 3. Sample fit (a) and the corresponding second derivative (b) for polymer PEGDA in D_2O with NaCl for varying weight %. Here, panel 1 is for 0%, panel 2 is for 20%, panel 3 is for 40%, panel 4 is for 60%, panel 5 is for 80%, and panel 6 is for 100%. In the top section of each panel the original FTIR spectrum is shown in blue, the sum of the two-Gaussian fit is shown in green, the 0 and 1 H-bond populations are shown in yellow and red respectively. The bottom panel displays the original FTIR spectrum second derivative in blue and the fitted spectrum is represented in red.

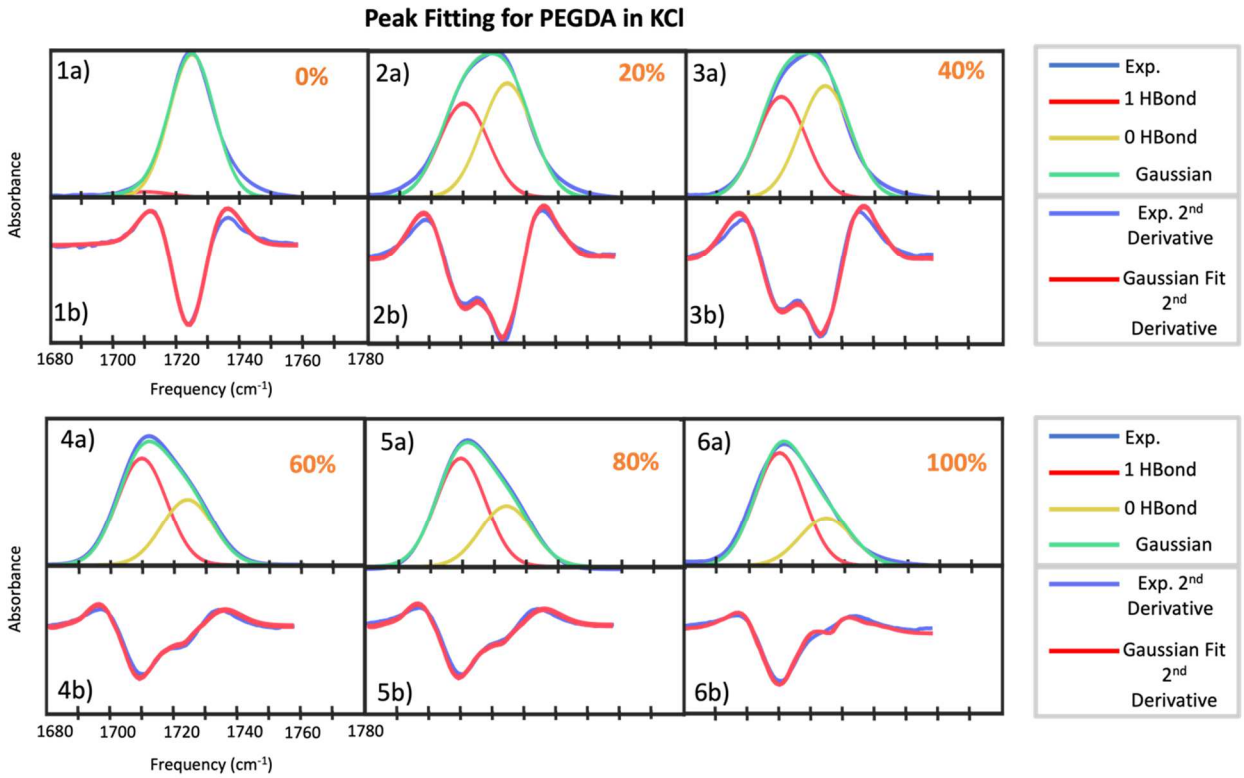

Figure 4. Sample fit (a) and the corresponding second derivative (b) for polymer PEGDA in D_2O with KCl for varying weight %. Here, panel 1 is for 0%, panel 2 is for 20%, panel 3 is for 40%, panel 4 is for 60%, panel 5 is for 80%, and panel 6 is for 100%. In the top section of each panel the original FTIR spectrum is shown in blue, the sum of the two-Gaussian fit is shown in green, the 0 and 1 H-bond populations are shown in yellow and red respectively. The bottom panel displays the original FTIR spectrum second derivative in blue and the fitted spectrum is represented in red.

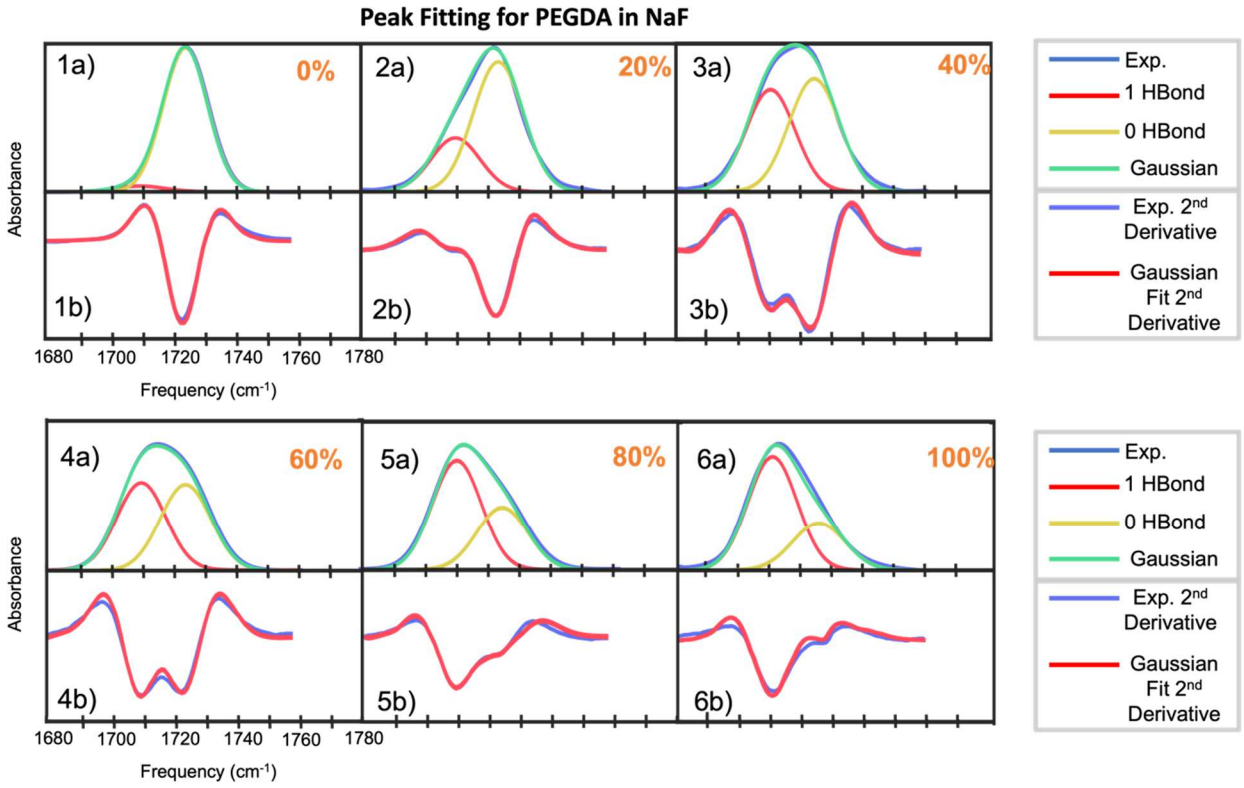

Figure 5. Sample fit (a) and the corresponding second derivative (b) for polymer PEGDA in D_2O with NaF for varying weight %. Here, panel 1 is for 0%, panel 2 is for 20%, panel 3 is for 40%, panel 4 is for 60%, panel 5 is for 80%, and panel 6 is for 100%. In the top section of each panel the original FTIR spectrum is shown in blue, the sum of the two-Gaussian fit is shown in green, the 0 and 1 H-bond populations are shown in yellow and red respectively. The bottom panel displays the original FTIR spectrum second derivative in blue and the fitted spectrum is represented in red.

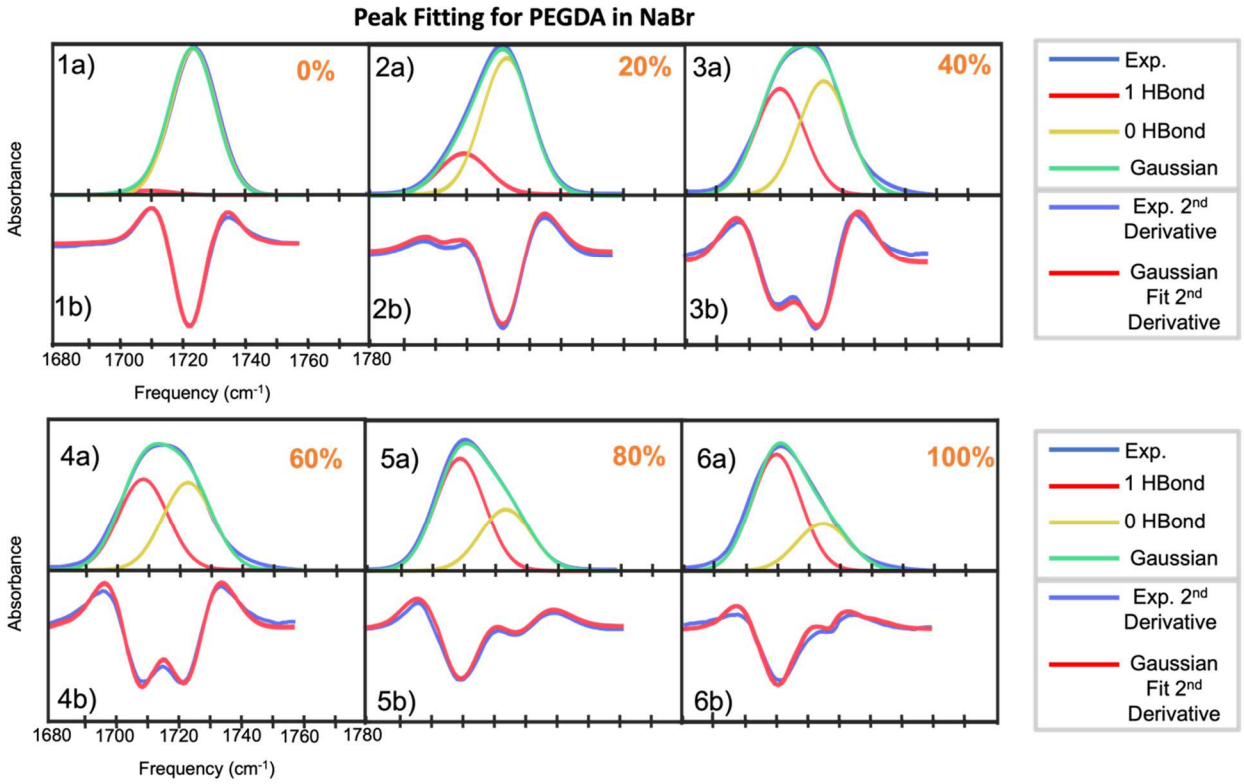

Figure 6. Sample fit (a) and the corresponding second derivative (b) for polymer PEGDA in D_2O with NaBr for varying weight %. Here, panel 1 is for 0%, panel 2 is for 20%, panel 3 is for 40%, panel 4 is for 60%, panel 5 is for 80%, and panel 6 is for 100%. In the top section of each panel the original FTIR spectrum is shown in blue, the sum of the two-Gaussian fit is shown in green, the 0 and 1 H-bond populations are shown in yellow and red respectively. The bottom panel displays the original FTIR spectrum second derivative in blue and the fitted spectrum is represented in red.

Salt 0%	Average Hydrogen Bond Population
LiCl	0.024 ± 0.011
NaCl	0.037 ± 0.011
KCl	0.048 ± 0.010
NaF	0.020 ± 0.011
NaBr	0.048 ± 0.012
Water	0.017 ± 0.009

Table 1. Hydrogen Bond Populations for 0% solutions.

Salt 20%	Average Hydrogen Bond Population
LiCl	0.110 ± 0.020
NaCl	0.250 ± 0.020
KCl	0.291 ± 0.022
NaF	0.150 ± 0.021
NaBr	0.333 ± 0.020
Water	0.077 ± 0.010

Table 2. Hydrogen Bond Populations for 20% solutions.

Salt 40%	Average Hydrogen Bond Population
LiCl	0.301 ± 0.020
NaCl	0.430 ± 0.019
KCl	0.491 ± 0.019
NaF	0.350 ± 0.020
NaBr	0.482 ± 0.021
Water	0.210 ± 0.009

Table 3. Hydrogen Bond Populations for 40% solutions.

Salt 60%	Average Hydrogen Bond Population
LiCl	0.444 ± 0.029
NaCl	0.493 ± 0.028
KCl	0.511 ± 0.028
NaF	0.455 ± 0.028
NaBr	0.510 ± 0.020
Water	0.362 ± 0.009

Table 4. Hydrogen Bond Populations for 60% solutions.

Salt 80%	Average Hydrogen Bond Population
LiCl	0.590 ± 0.031
NaCl	0.607 ± 0.032
KCl	0.668 ± 0.033
NaF	0.601 ± 0.033
NaBr	0.623 ± 0.033
Water	0.451 ± 0.008

Table 5. Hydrogen Bond Populations for 80% solutions.

Salt 100%	Average Hydrogen Bond Population
LiCl	0.598 ± 0.027
NaCl	0.610 ± 0.026
KCl	0.683 ± 0.025
NaF	0.611 ± 0.025
NaBr	0.668 ± 0.024
Water	0.555 ± 0.010

Table 6. Hydrogen Bond Populations for 100% solutions.

SI.2 2D IR Spectroscopy

In 2D IR spectroscopy, CLS is a crucial metric used to extract information about the timescale of frequency fluctuations of molecular vibrations, which is directly related to the dynamics of the system, such as hydrogen bond lifetimes. The CLS is obtained by analyzing the diagonal contour lines of the 2D IR spectrum at different waiting times (t2). This slope provides insight into the frequency-frequency correlation function, which reflects how vibrational frequencies change over time due to the dynamic environment. In simpler terms, a higher CLS value (closer to 1) at shorter waiting times indicates that the vibrational frequency of a mode is highly correlated over time, suggesting that the environment around the vibration is relatively stable. As the waiting time increases, the CLS value typically decays toward zero, indicating that the correlation has diminished and that the environment has changed, which in our context relates to hydrogen bond dynamics.

The decay of the CLS over time can be modeled with an exponential decay function, providing a timescale for the frequency fluctuations, which corresponds to the lifetime of the hydrogen bond dynamics in the system. This information is critical for understanding how different ions affect the stability and dynamics of hydrogen bonds in the polymer matrix. For example, the difference in CLS behavior for F^- compared to Na^+ indicates differing impacts on the hydrogen bond lifetimes, with the CLS value reflecting how quickly these bonds are forming and breaking under different ionic conditions.

In our experiment, the center line slope (CLS) fits to each spectrum produces the timescale of the frequency-fluctuations of the surfactant ester carbonyl. The CLS was calculated through analysis of the 0 H-Bond peak and 1 H-Bond peak for each sample at different waiting times (t_2). As there are two features overlapped in our absorption peak, we explored the lower and high frequency halves of each feature. The CLS fits have significant uncertainties due to the relatively narrow frequency region analyzed compared to the entire peak. However, the results are consistent for different samples, which provides confidence in the timescales extracted. The waiting-time dependent CLS was fit to an exponential decay with an offset (**Eq. 2**):

$$CLS(t_2) = ae^{-\left(\frac{t_2}{b}\right)} + c \tag{2}$$

The wavenumber region used for CLS analysis was determined through full-width half-maximum of the FTIR Gaussian fits. With this initial range determined, we choose a smaller wavenumber subset that was used for the fitting of the zero and one hydrogen bond for all salts that resulted in cleaner CLS fitting. Different methods for CLS and nodal-line slope (NLS) analysis were done and all methods resulted in the same trends. We do not report or discuss the high-frequency zero hydrogen bond feature further as reliable results could not be obtained.

	0%	50%	100%
Zero Hydrogen Bond	1719-1725 cm^{-1}	1714-1726 cm^{-1}	1713-1726 cm^{-1}
One Hydrogen Bond	1711-1718 cm^{-1}	1706-1712 cm^{-1}	1705-1711 cm^{-1}

Table 7. Parameters for fitting 2D IR in CLS fitting.

SI.3 CLS Analysis

The following tables present the CLS exponential decay constants. For the hydrogen bond dynamics in the 0% solutions for both cations and anions, you will see "N/A" since there is no decay within the timescale of the measurement. This is because these solutions contain no water, and therefore, no hydrogen bond dynamics occur with the ester carbonyl group. Additionally, we provide the CLS offset but do not discuss this metric since, unlike the time constant, the values of the offset depend on the frequency region selected.

To ensure the accuracy and to obtain a statistical uncertainty of the extracted timescales, the CLS is computed using bootstrapping, where 50% of the points are randomly removed and the fit is re-computed across several iterations. The average and the standard deviation of the distribution of fit parameters is reported.

Cations 1 Hbond Lifetime (ps)	0%	50%	100%
LiCl	N/A	0.58 ± 0.30	1.52 ± 0.31
NaCl	N/A	0.40 ± 0.25	1.39 ± 0.40
KCl	N/A	0.28 ± 0.15	1.09 ± 0.31

Table 8. Decay constants for the one hydrogen bond feature for cations obtained through CLS fitting of 2D IR spectra.

Cations 1 Hbond CLS Offset	0%	50%	100%
LiCl	N/A	0.60 ± 0.03	0.28 ± 0.04
NaCl	N/A	0.57 ± 0.02	0.27 ± 0.03
KCl	N/A	0.58 ± 0.02	0.22 ± 0.07

Table 9. CLS offset for the one hydrogen bond feature for cations obtained through CLS fitting of 2D IR spectra.

Anions 1 Hbond Lifetime (ps)	0%	50%	100%
NaF	N/A	0.63 ± 0.32	1.94 ± 0.47
NaCl	N/A	0.40 ± 0.25	1.39 ± 0.40
NaBr	N/A	0.24 ± 0.17	0.77 ± 0.19

Table 10. Decay constants for the one hydrogen bond feature for anions obtained through CLS fitting of 2D IR spectra.

Anions 1 Hbond CLS Offset	0%	50%	100%
NaF	N/A	0.62 ± 0.04	0.14 ± 0.05
NaCl	N/A	0.57 ± 0.02	0.27 ± 0.03
NaBr	N/A	0.56 ± 0.01	0.44 ± 0.06

Table 11. CLS offset for the one hydrogen bond feature for anions obtained through CLS fitting of 2D IR spectra.

<u>For 0% Solutions: NaF</u>

a. One hydrogen bond feature

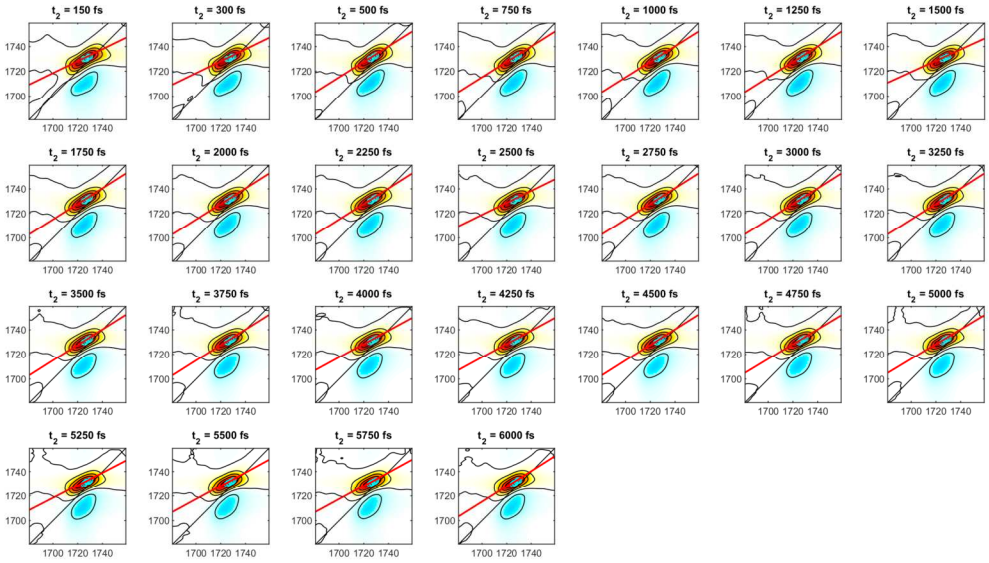

Figure 7. 2D IR spectra of 0% NaF at 25˚C fitting the one hydrogen bond peak feature. The horizontal axis is the excitation axis, and the vertical axis is detection axis. The red line is the CLS fit. The waiting time (t2) is shown above each spectrum.

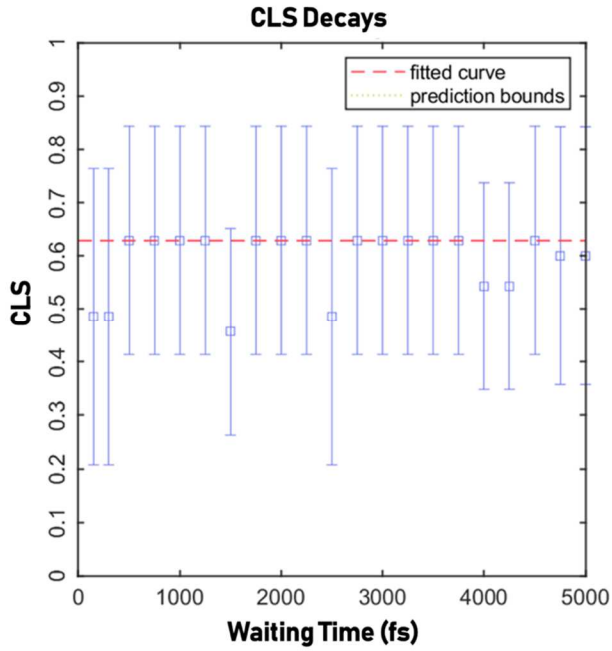

Figure 8. CLS Decay fitting for 0%NaF fitting the one hydrogen bond peak feature.

For 0% Solutions: LiCl

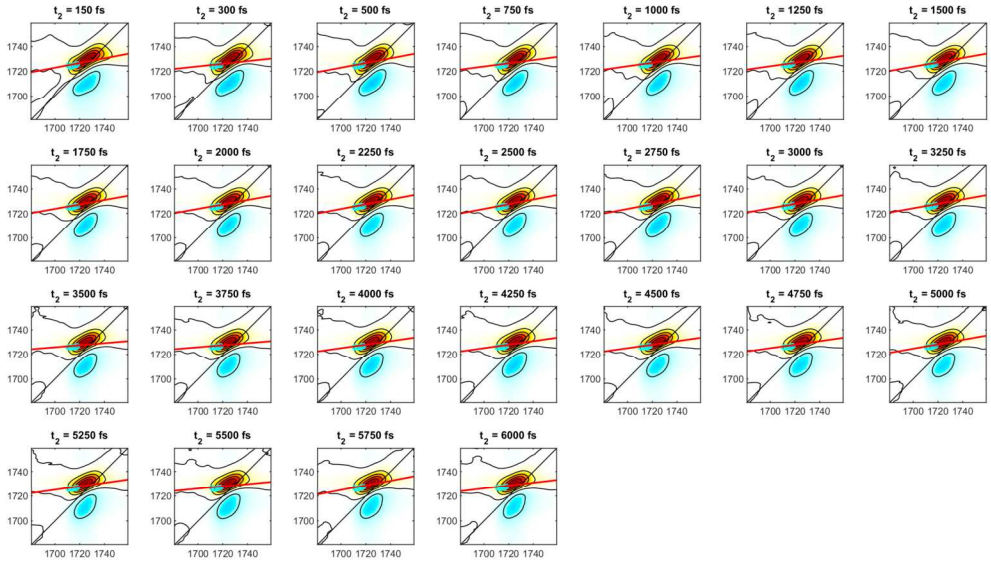

Figure 9. 2D IR spectra of 0% LiCl at 25˚C fitting the one hydrogen bond peak feature. The horizontal axis is the excitation axis, and the vertical axis is detection axis. The red line is the CLS fit. The waiting time (t2) is shown above each spectrum.

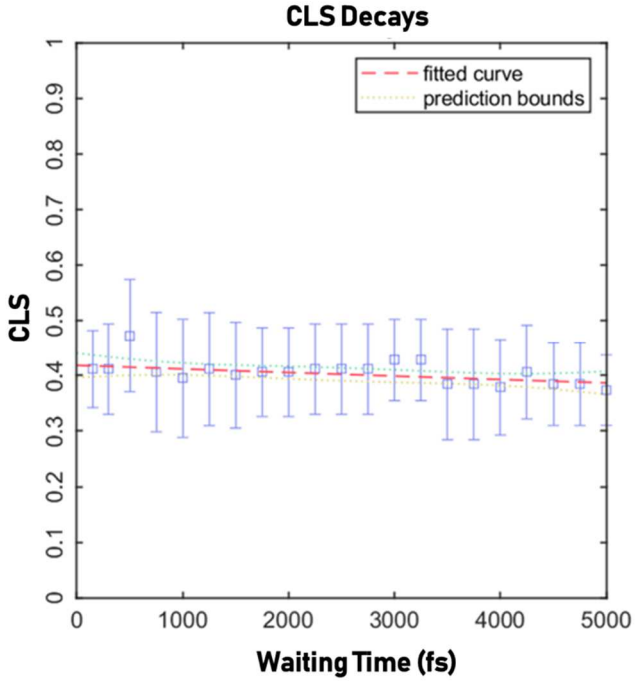

Figure 10. CLS Decay fitting for 0% LiCl fitting the one hydrogen bond peak feature.

For 0% Solutions: NaCl

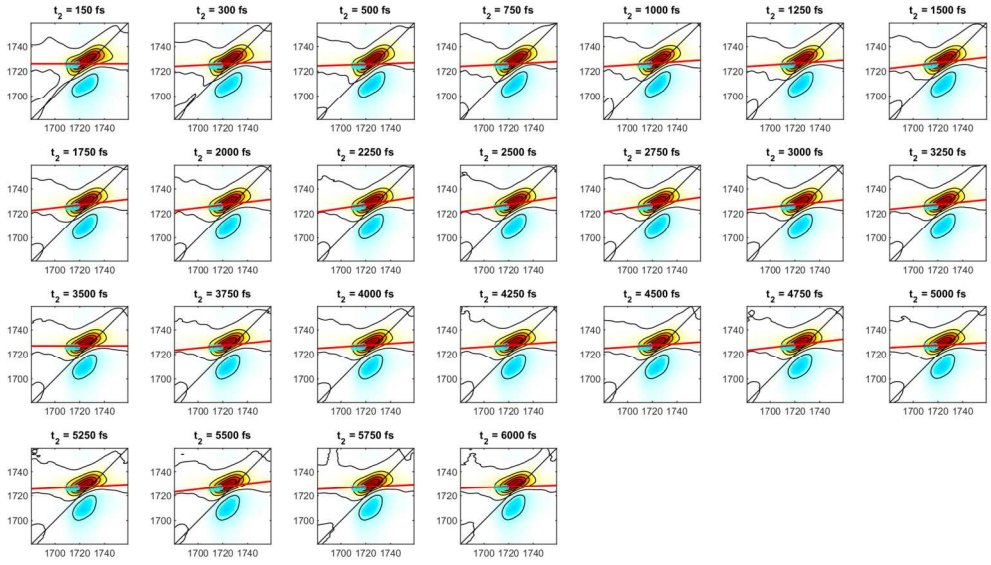

Figure 11. 2D IR spectra of 0% NaCl at 25˚C fitting the one hydrogen bond peak feature. The horizontal axis is the excitation axis, and the vertical axis is detection axis. The red line is the CLS fit. The waiting time (t2) is shown above each spectrum.

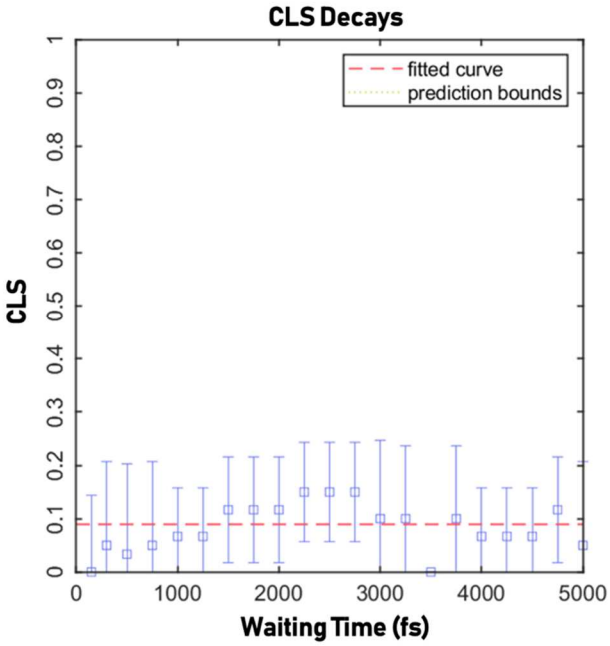

Figure 12. CLS Decay fitting for 0% NaCl fitting the one hydrogen bond peak feature.

For 0% Solutions: NaBr

a. One hydrogen bond feature

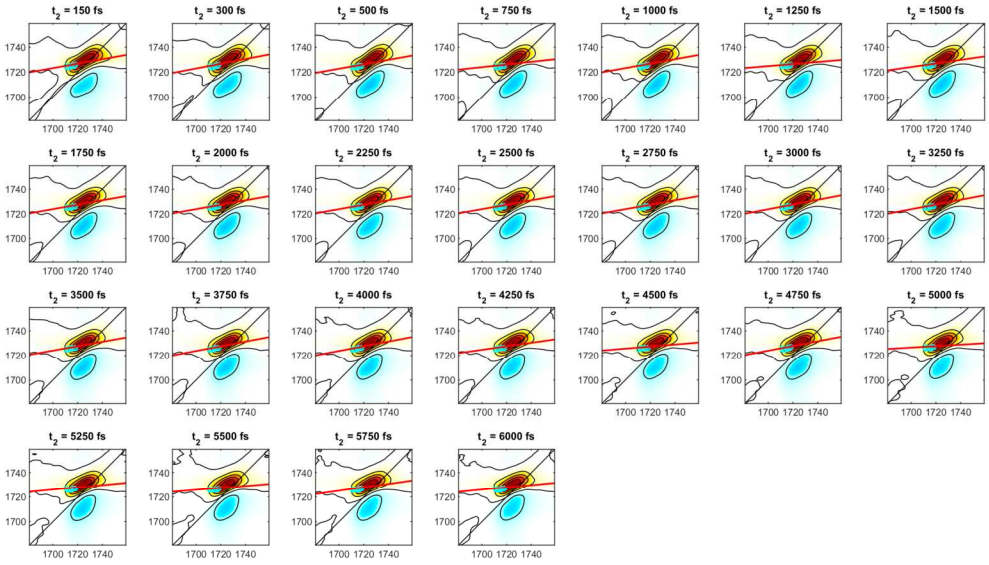

Figure 13. 2D IR spectra of 0% NaBr at 25˚C fitting the one hydrogen bond peak feature. The horizontal axis is the excitation axis, and the vertical axis is detection axis. The red line is the CLS fit. The waiting time (t2) is shown above each spectrum.

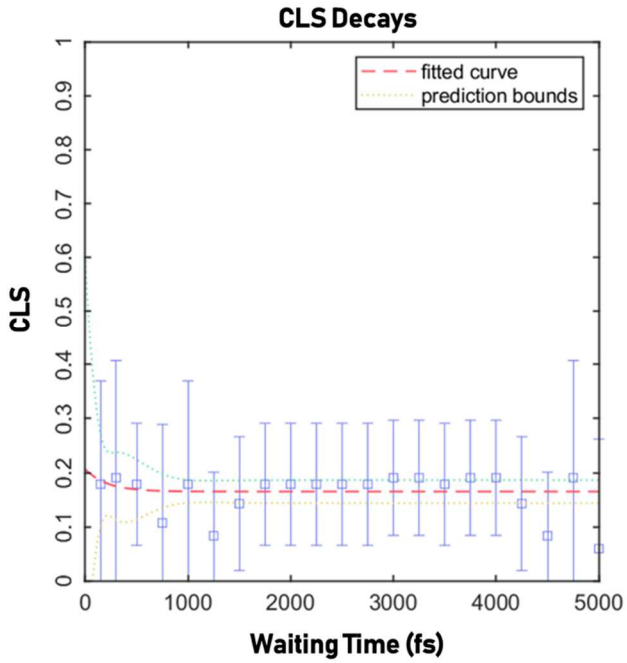

Figure 14. CLS Decay fitting for 0% NaBr fitting the one hydrogen bond peak feature.

For 0% Solutions: KCl

a. One hydrogen bond feature

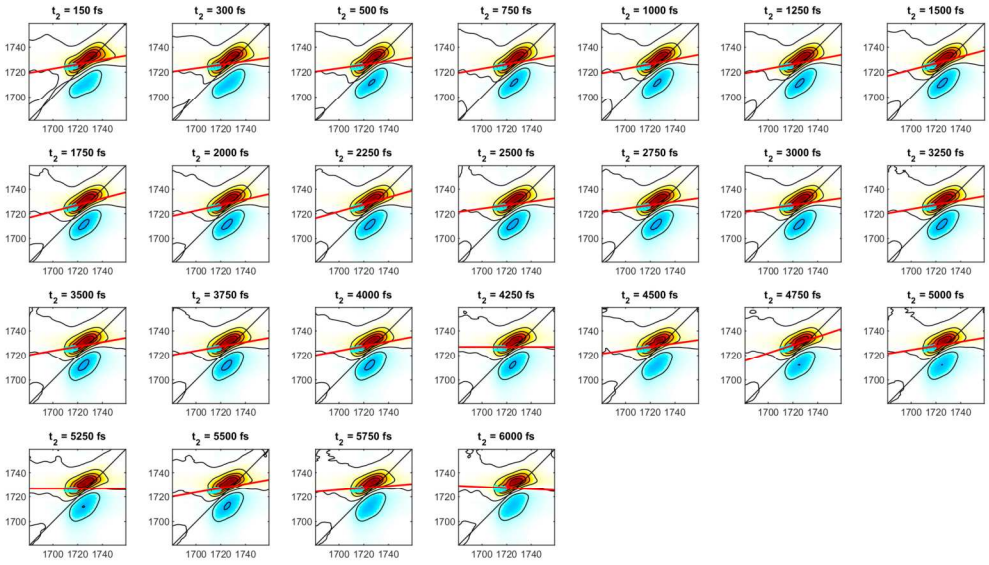

Figure 15. 2D IR spectra of 0% KCl at 25˚C fitting the one hydrogen bond peak feature. The horizontal axis is the excitation axis, and the vertical axis is detection axis. The red line is the CLS fit. The waiting time (t2) is shown above each spectrum.

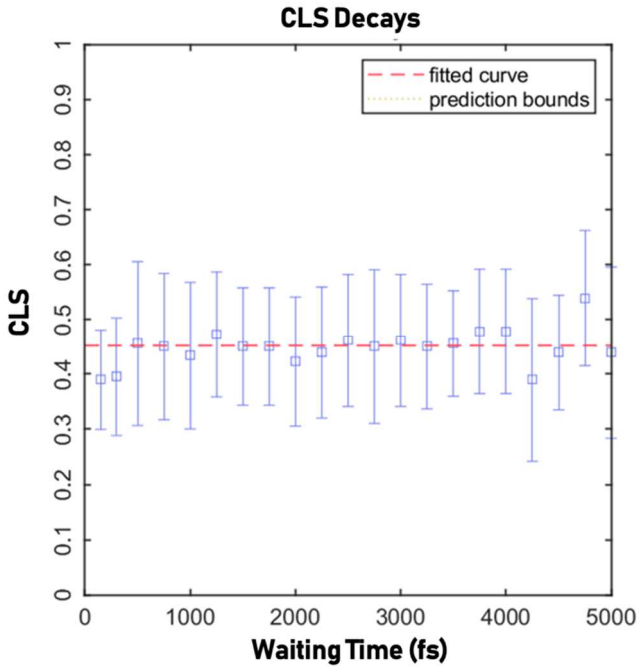

Figure 16. CLS Decay fitting for 0% KCl fitting the one hydrogen bond peak feature.

For 50% Solutions: NaF

b. One hydrogen bond feature

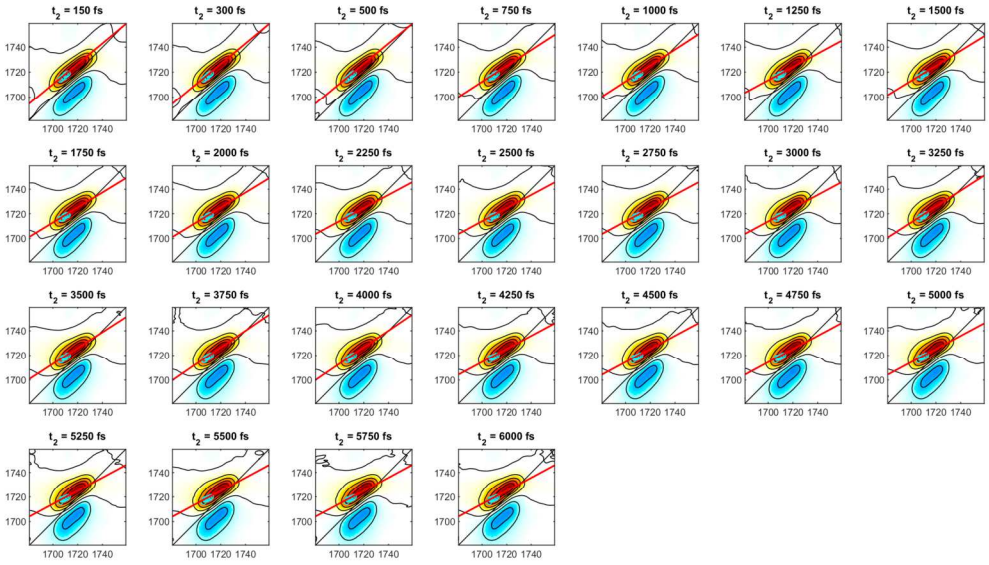

Figure 17. 2D IR spectra of 50% NaF at 25˚C fitting the one hydrogen bond peak feature. The horizontal axis is the excitation axis, and the vertical axis is detection axis. The red line is the CLS fit. The waiting time (t2) is shown above each spectrum.

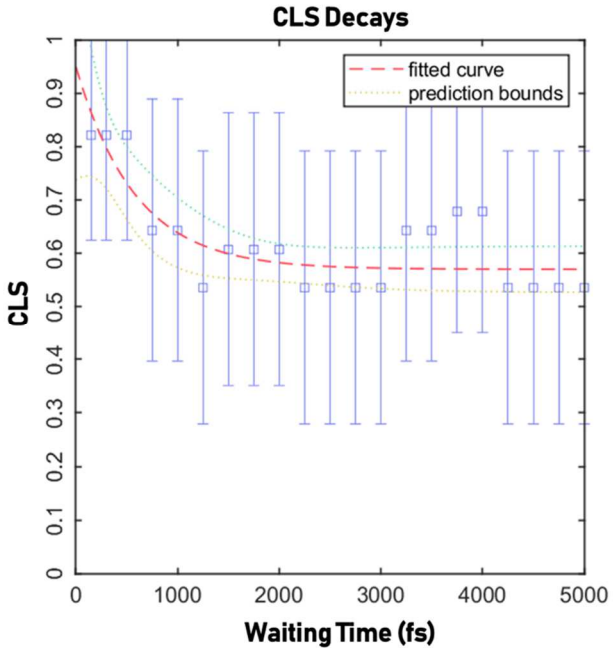

Figure 18. CLS Decay fitting for 50% NaF fitting the one hydrogen bond peak feature.

For 50% Solutions: LiCl

a. One hydrogen bond feature

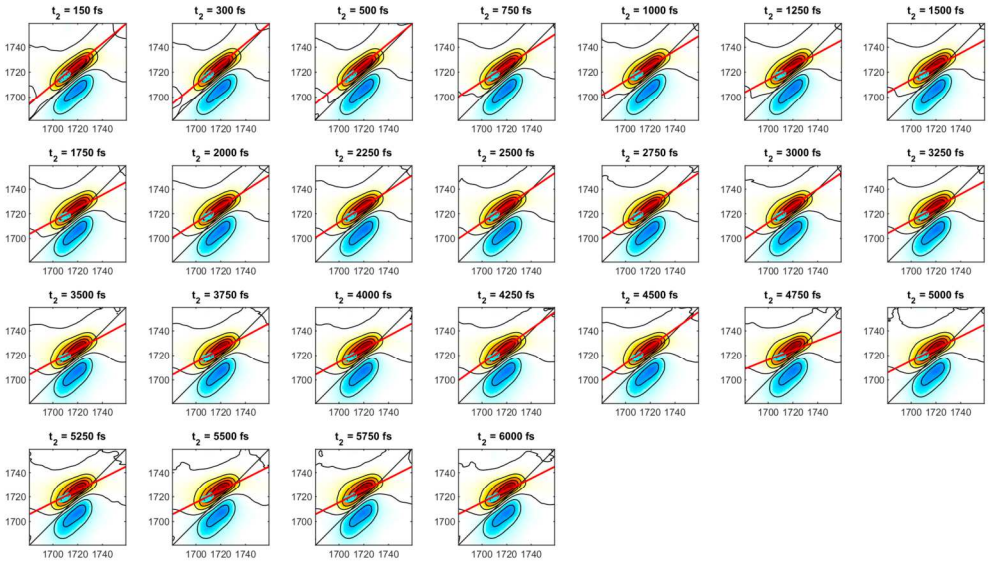

Figure 19. 2D IR spectra of 50% LiCl at 25˚C fitting the one hydrogen bond peak feature. The horizontal axis is the excitation axis, and the vertical axis is detection axis. The red line is the CLS fit. The waiting time (t2) is shown above each spectrum.

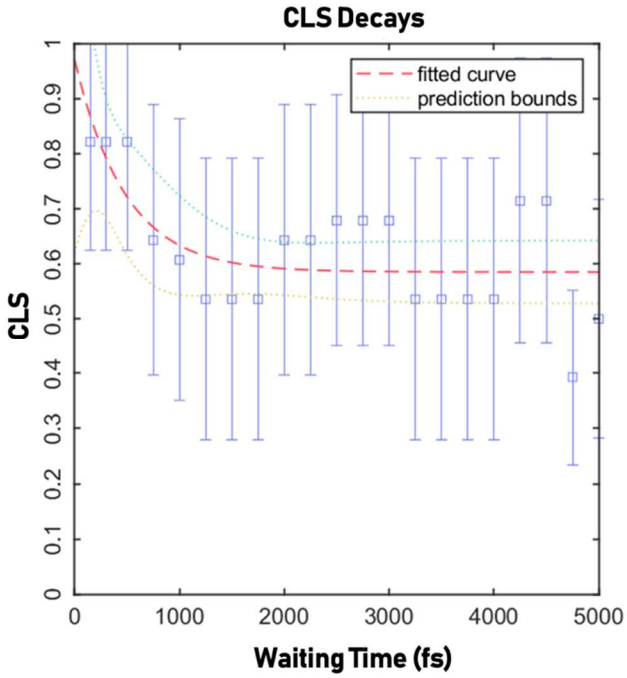

Figure 20. CLS Decay fitting for 50% LiCl fitting the one hydrogen bond peak feature.

For 50% Solutions: NaCl

a. One hydrogen bond feature

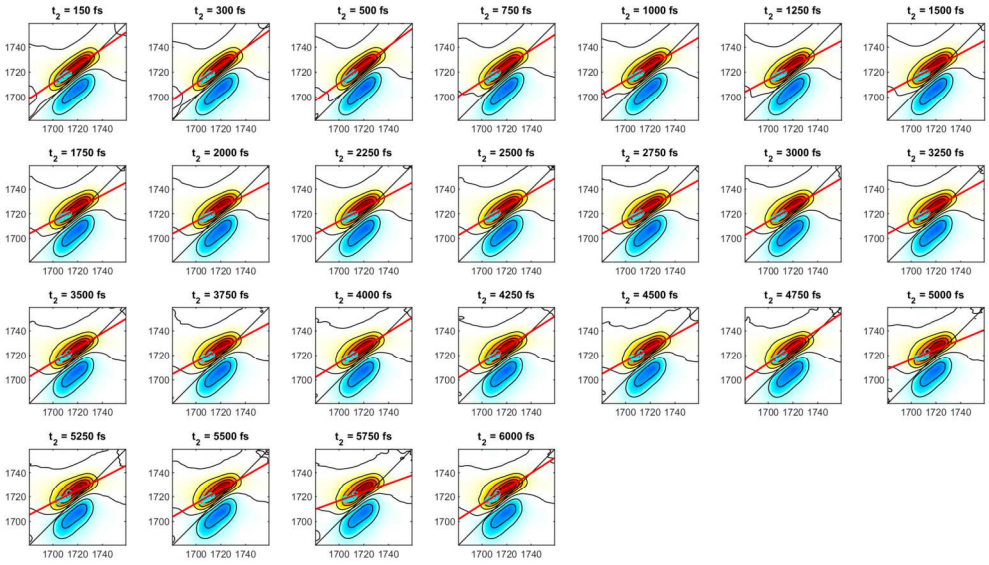

Figure 21. 2D IR spectra of 50% NaCl at 25˚C fitting the one hydrogen bond peak feature. The horizontal axis is the excitation axis, and the vertical axis is detection axis. The red line is the CLS fit. The waiting time (t2) is shown above each spectrum.

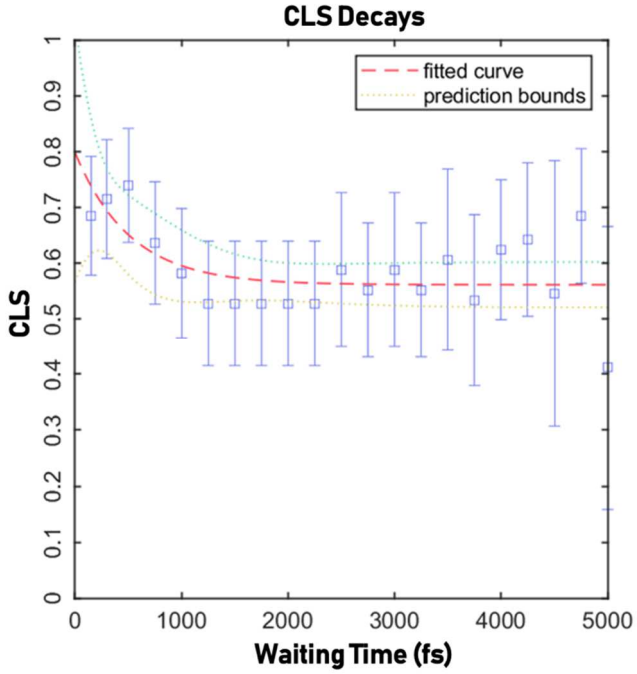

Figure 22. CLS Decay fitting for 50% NaCl fitting the one hydrogen bond peak feature.

For 50% Solutions: NaBr

b. One hydrogen bond feature

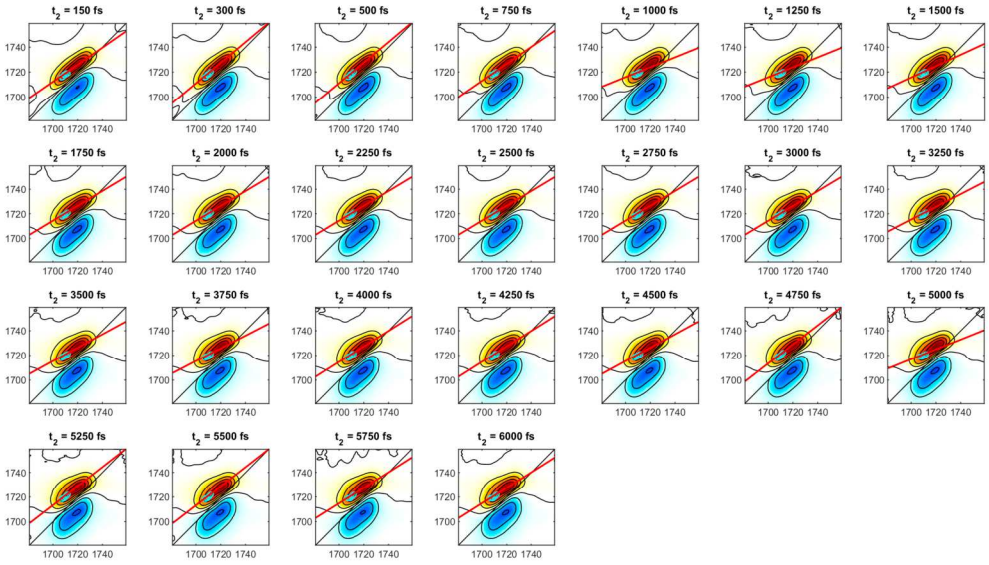

Figure 23. 2D IR spectra of 50% NaBr at 25˚C fitting the one hydrogen bond peak feature. The horizontal axis is the excitation axis, and the vertical axis is detection axis. The red line is the CLS fit. The waiting time (t2) is shown above each spectrum.

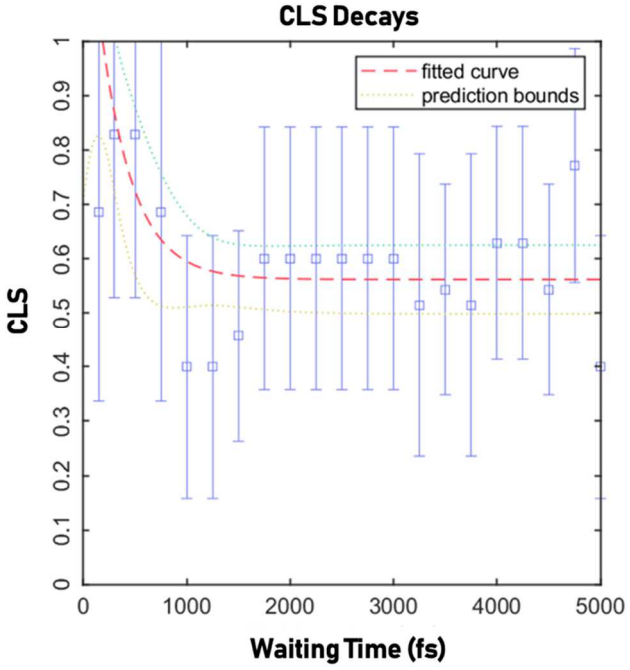

Figure 24. CLS Decay fitting for 50% NaBr fitting the one hydrogen bond peak feature.

For 50% Solutions: KCl

b. One hydrogen bond feature

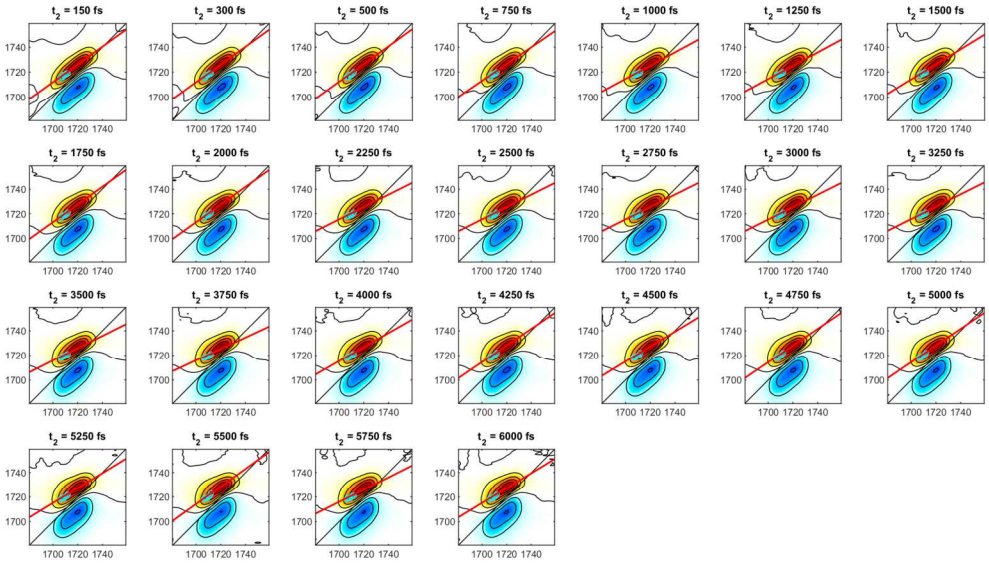

Figure 25. 2D IR spectra of 50% KCl at 25˚C fitting the one hydrogen bond peak feature. The horizontal axis is the excitation axis, and the vertical axis is detection axis. The red line is the CLS fit. The waiting time (t2) is shown above each spectrum.

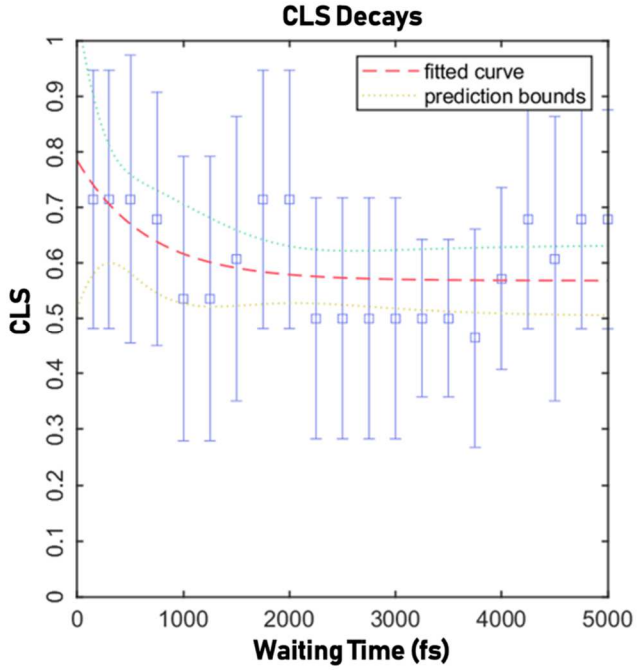

Figure 26. CLS Decay fitting and constant for 50% KCl fitting the one hydrogen bond peak feature.

For 100% Solutions: NaF

c. One hydrogen bond feature

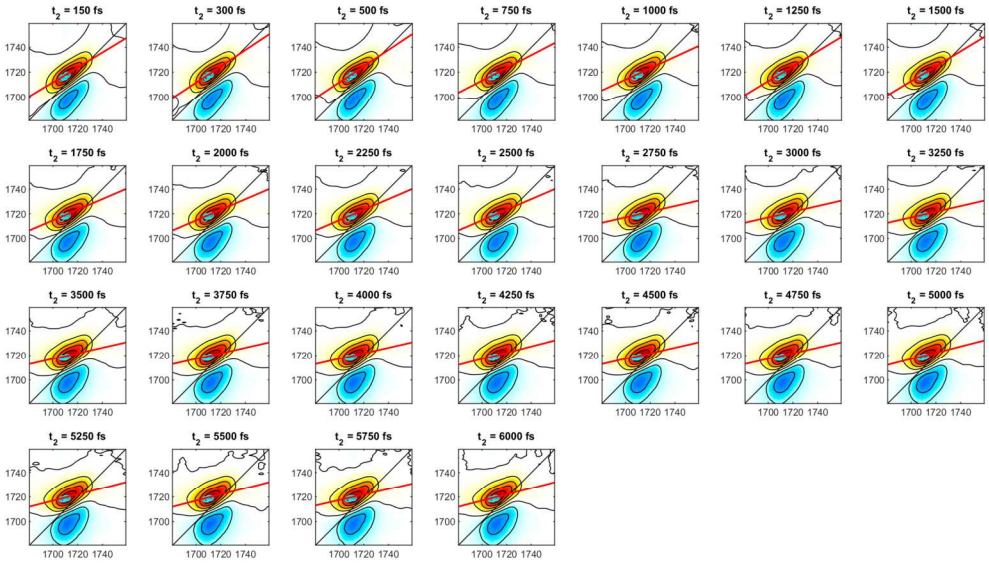

Figure 27. 2D IR spectra of 100% NaF at 25˚C fitting the one hydrogen bond peak feature. The horizontal axis is the excitation axis, and the vertical axis is detection axis. The red line is the CLS fit. The waiting time (t2) is shown above each spectrum.

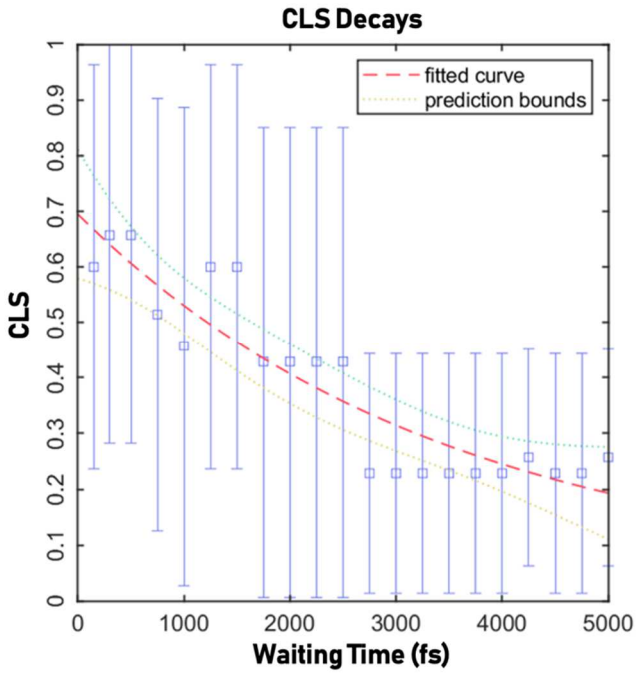

Figure 28. CLS Decay fitting 100% NaF fitting the one hydrogen bond peak feature.

For 100% Solutions: LiCl

b. One hydrogen bond feature

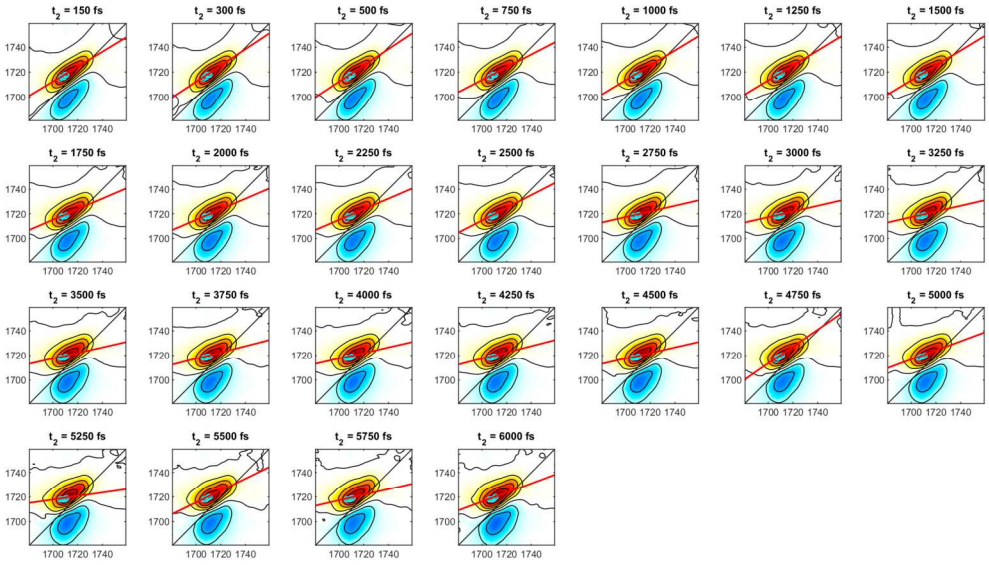

Figure 29. 2D IR spectra of 100% LiCl at 25˚C fitting the one hydrogen bond peak feature. The horizontal axis is the excitation axis, and the vertical axis is detection axis. The red line is the CLS fit. The waiting time (t2) is shown above each spectrum.

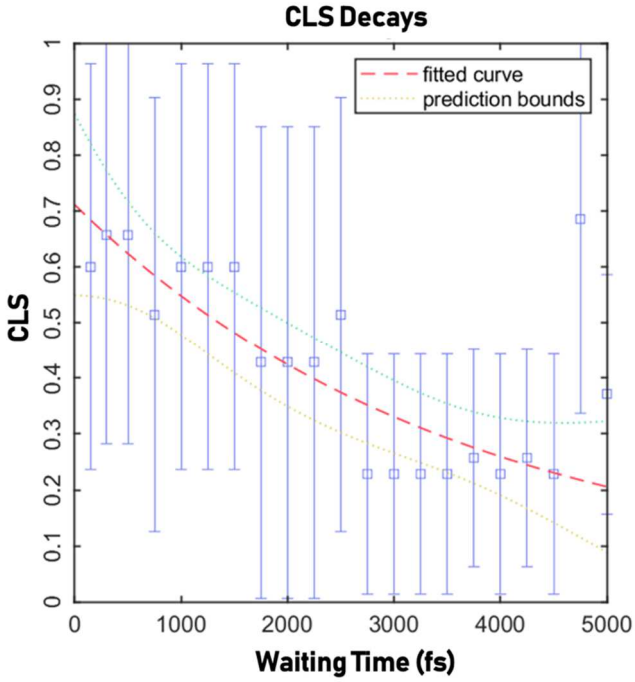

Figure 30. CLS Decay fitting for 100% LiCl fitting the one hydrogen bond peak feature.

For 100% Solutions: NaCl

b. One hydrogen bond feature

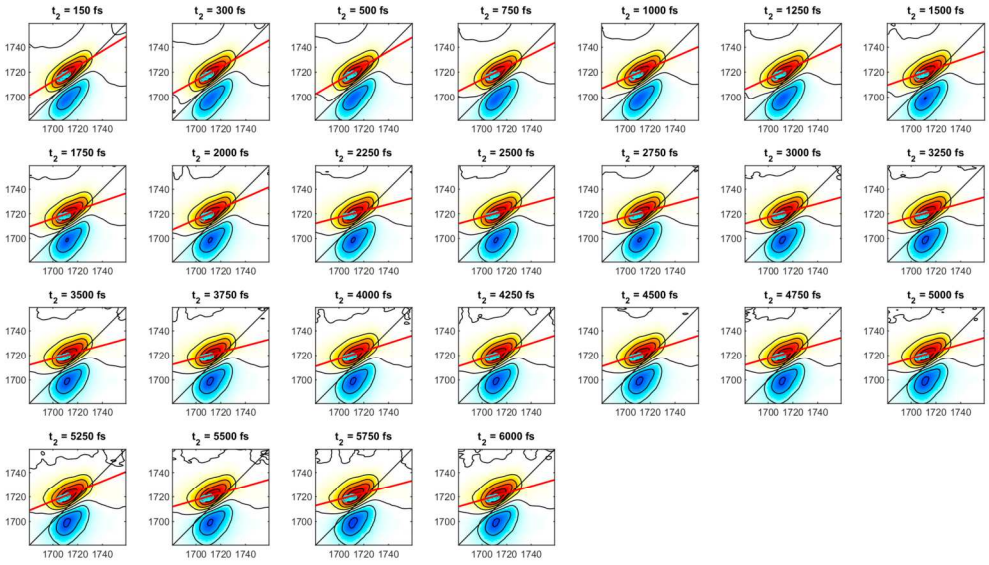

Figure 31. 2D IR spectra of 100% NaCl at 25˚C fitting the one hydrogen bond peak feature. The horizontal axis is the excitation axis, and the vertical axis is detection axis. The red line is the CLS fit. The waiting time (t2) is shown above each spectrum.

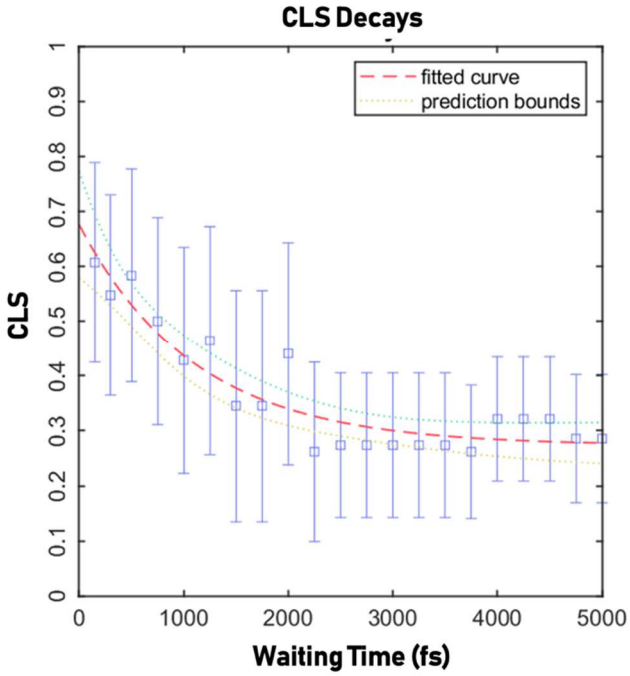

Figure 32. CLS Decay fitting for 100% NaCl fitting the one hydrogen bond peak feature.

For 100% Solutions: NaBr

c. One hydrogen bond feature

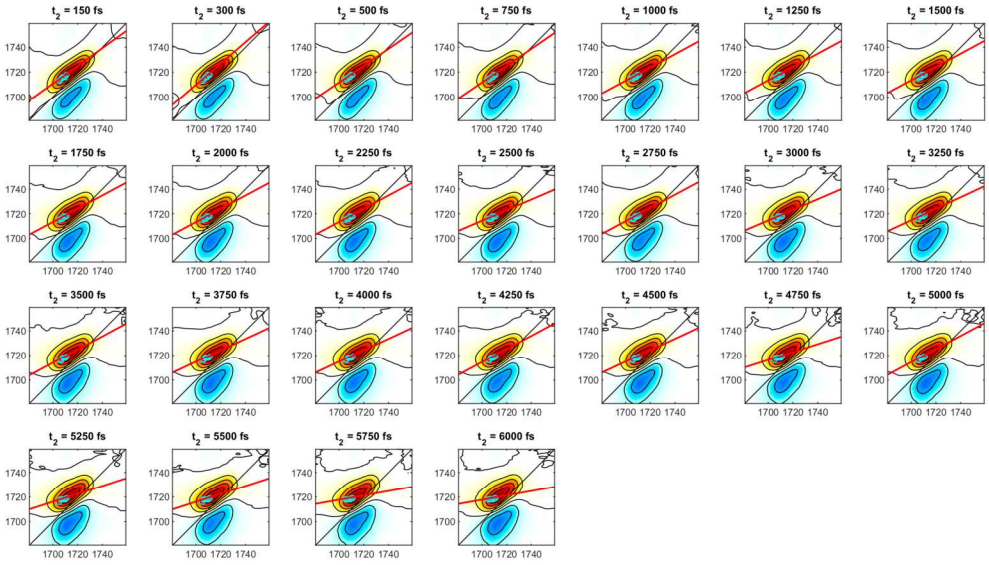

Figure 33. 2D IR spectra of 100% NaBr at 25˚C fitting the one hydrogen bond peak feature. The horizontal axis is the excitation axis, and the vertical axis is detection axis. The red line is the CLS fit. The waiting time (t2) is shown above each spectrum.

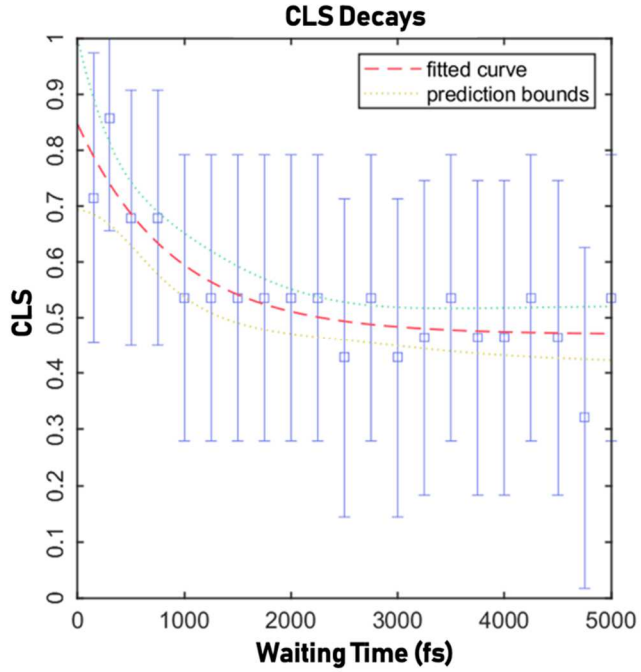

Figure 34. CLS Decay fitting for 100% NaBr fitting the one hydrogen bond peak feature

For 100% Solutions: KCl

c. One hydrogen bond feature

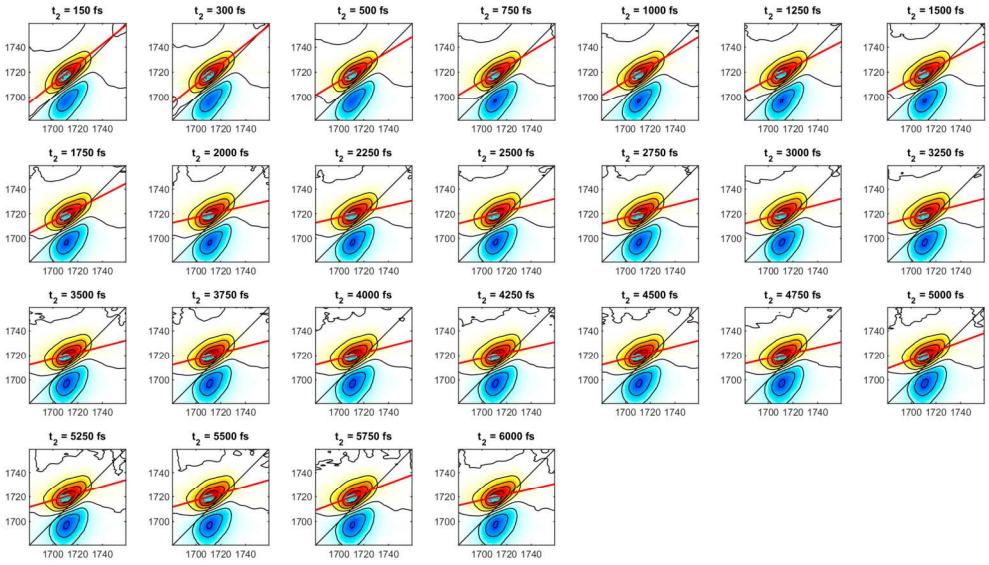

Figure 35. 2D IR spectra of 100% KCl at 25˚C fitting the one hydrogen bond peak feature. The horizontal axis is the excitation axis, and the vertical axis is detection axis. The red line is the CLS fit. The waiting time (t2) is shown above each spectrum.

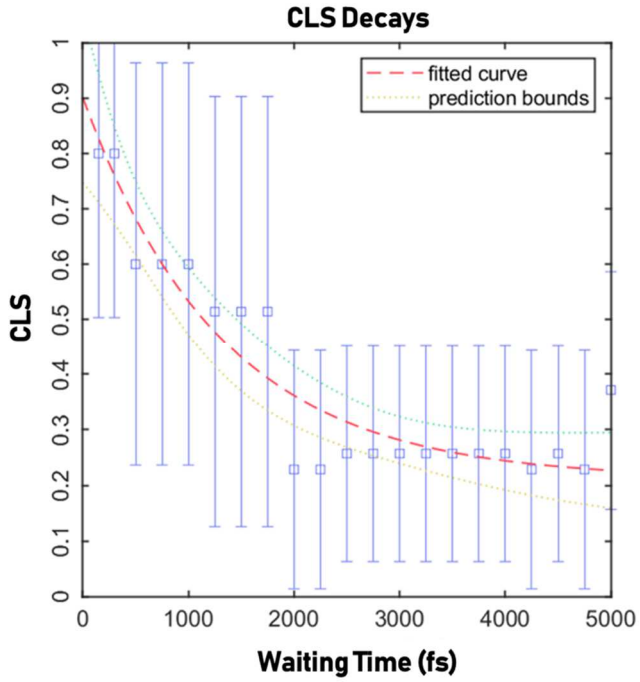

Figure 36. CLS Decay fitting for 100% KCl fitting the one hydrogen bond peak feature.

SI.4 Validation for CLS Analysis

In 2D IR spectroscopy, chemical exchange refers to the process where molecules switch between different states or environments, such as between different hydrogen-bonding configurations. When chemical exchange occurs on a timescale that is comparable to the waiting time (t2) in a 2D IR experiment, it often results in cross-peaks in the 2D IR spectrum. These cross-peaks indicate that a molecule excited in one state (e.g., a free carbonyl or 0-HB state) has transitioned to another state (e.g., a hydrogen-bonded or 1-HB state) during the experiment.

The absence of cross-peaks in your spectra could indicate that chemical exchange between states is not occurring on a timescale that is detectable in your experiment. However, this does not necessarily mean that there are no dynamics in the system. The system may still be dynamic, but the transitions between states might be occurring too quickly (faster than the experimental resolution) or too slowly (longer than the waiting time t2 used in the experiment) to be detected as cross-peaks.

Even without cross-peaks, the dynamics of the system can still be probed using CLS analysis. The CLS method tracks how the vibrational frequency of a mode (such as the 1-HB peak) evolves over time. The decay of the CLS over different waiting times provides information about how the environment around the vibrational mode is changing, which is related to the breaking and reforming of hydrogen bonds. This decay gives insights into the hydrogen bond lifetimes and the overall dynamics of the system.

In systems where chemical exchange is either too fast or too slow to be resolved as cross-peaks, CLS analysis becomes particularly valuable. It provides a measure of how dynamic processes, such as hydrogen bond fluctuations, influence the vibrational modes, even if the direct evidence of state exchange (cross-peaks) is not visible. Therefore, while cross-peaks provide direct evidence of exchange, the absence of cross-peaks does not negate the presence of dynamic processes; it merely shifts the emphasis to different analytical methods like CLS to extract relevant information.

In support of our analysis and interpretation using CLS in 2D IR spectroscopy, we have conducted similar studies in other systems where hydrogen bond dynamics were explored using this method.[2–4] These studies further validate the robustness of CLS as a method for probing dynamic processes in systems where direct observation of chemical exchange via cross-peaks is not feasible. Our consistent findings across these studies reinforce the reliability of CLS analysis in capturing the essential dynamics of hydrogen bonding within various environments.

References:

(1) Valentine, M. L.; Waterland, M. K.; Fathizadeh, A.; Elber, R.; Baiz, C. R. Interfacial Dynamics in Lipid Membranes: The Effects of Headgroup Structures. *J. Phys. Chem. B* **2021**, *125* (5), 1343–1350. https://doi.org/10.1021/acs.jpcb.0c08755.
(2) Garrett, P.; Baiz, C. R. Dynamic Effect of Polymers at the Surfactant–Water Interface: An Ultrafast Study. *Soft Matter* **2022**, *18* (9), 1793–1800. https://doi.org/10.1039/D1SM01651B.
(3) Garrett, P.; Baiz, C. R. Hidden Beneath the Layers: Extending the Core/Shell Model of Reverse Micelles. *J. Phys. Chem. B* **2023**, *127* (43), 9399–9404. https://doi.org/10.1021/acs.jpcb.3c04978.
(4) Garrett, P.; Shirley, J. C.; Baiz, C. R. Forced Interactions: Ionic Polymers at Charged Surfactant Interfaces. *J. Phys. Chem. B* **2023**, *127* (12), 2829–2836. https://doi.org/10.1021/acs.jpcb.2c08636.